Available online www.jsaer.com

***Journal of Scientific and Engineering Research*, 2018, 5(7):119-135**

Research Article

ISSN: 2394-2630
CODEN(USA): JSERBR

Stability Analysis of a Kelvin-Helmholtz Flow of an Electrified Horizontal Sheet through Porous Media

G.M. Moatimid[1], N.T. El-dabe[1], A. Sayed[2]

[1]Department of Mathematics, Faculty of Education, Ain Shams University, Roxy, Cairo, Egypt
[2]Department of Mathematics, Faculty of Sciences, Beni-Seuf University, Beni-Seuf, Egypt

Abstract In the current article, a stability of double interfaces between three incompressible, viscous, and incompressible finite layers is investigated. The fluids are saturated through media. The system is influenced by a uniform tangential electric field. The analysis is based on the viscous potential theory, which considered that the influence of the viscous forces is affected only at the interfaces. Meanwhile, away from the interfaces, the fluids behave like inviscid ones. On using the normal modes analysis, the boundary-value problem resulted in a second-order coupled differential equations with damping and complex coefficients. The Routh-Hurwitz criteria are adapted to govern the stability analysis. Several special cases are recovered in accordance with appropriate data choices. The stability criteria are analyzed theoretically and illustrated graphically. Regions of stability and instability are identified at which the electric field intensity is plotted versus the wave number of the surface waves. The influences of various parameters, of the problem at hand, on the stability of the wave train of the disturbance are graphed. It is found that the Darcy's coefficients, the dynamic viscosity and streaming flow play a destabilizing effect. In contrast, the thickness of the sheet and the porosity has a dual role in the stability picture.

Keywords Linear Stability, Electric Field, Porous Media, Viscous Potential Flow

Introduction

Rayleigh-Taylor instability (RTI) occurs when a heavy fluid is supported by a lighter one. Because of the wide applications of RTI, in planetary and stellar atmospheres etc., several studied have been addressed. Kelvin-Helmholtz instability (KHI) arises when two fluids are in a relative motion. The phenomenon of KHI is an important concept in understanding a variety of space, astrophysical and geophysical aspects. A good amount of the hydrodynamic stability for RIT, KHI and other has been reported through the pioneer book of Chandrasekhar [1]. The stability conditions of an electrified viscous fluid sheet are investigated by Moatimid [2]. Because of the complexity of the mathematical analysis, he considered a weak viscous effects, so that their contributions are incorporated only at the boundary conditions. He found that the sheet thickness has a dual role in the stability picture. The electrohydrodynamic stability of a fluid sheet is early studied by Elshehawey et al. [3]. In their analysis, the dielectric liquid sheet is stressed by gravitational force and a tangential periodic electric field. They showed that the two interfaces are governed by two simultaneous second-order differential equations. They do not apply the symmetric and anti-symmetric perturbations. Eltayeb and Loper [4] investigated the stability of two parallel interfaces. In their work, the stability of the interfaces is analyzed,first, in the limit that they are closed together, then for general spacing. They found that the interfaces are unstable for some wave number for all values of the Prandtle number and the interface spacing. An excellent book on the stability theory is given by Drazin and Reid [5]. They reported the analysis of RHI, KHI and capillary instability of perfect fluids.

The flow through porous media is of considerable interest in petroleum extracting and geophysical fluid dynamists. The linear KHI of parallel flow in porous media is analyzed by Bau [6]. He derived the instability conditions in KHI for Darcian and non-Darcian flows. Also, in both cases, the velocities should exceed some critical values in order to the instability to manifest it. The temporal stability of superposed magnetic fluids in porous media is investigated by Zakaria et al. [7]. Their system is composed of a middle fluid sheet of finite thickness and embedded between two other bounded layers. They found that the fluid sheet thickness plays a destabilizing role in case of uniform fields. In contrast of their analysis, the present work considers the influence of the porosity of the media. Alkharashi [8] studied the electrohydrodynamic instability of three dielectric fluids through porous media. In his article, he considered the basic streaming on the three layers is periodic. Therefore, he used the multiple time scale technique to achieve the stability analysis. At the same time, he ignored the influence of uniform streaming. Through the current paper, the same model is considered but in case of a uniform streaming. The following analysis reveals several special cases and studied the stability analysis in detail. In a subsequent paper, we will consider the periodicity of the streaming velocities to treat the different mistakes in his previous work [7]. The electrohydrodynamic KHI of two miscible ferrofluids in porous media is investigated by Moatimid [9]. He analyzed the linear as well as nonlinear aspects of stability theory of the interface between two superposed magnetic fluids. His stability criterion is obtained in terms of the competing parameter of the problem. Moatimid and Hassan [10] studied the instability of an electrohydrodynamic viscous liquid micro-cylinder buried in a porous media. Their analysis resulted in a transcendental dispersion relation. They found that the existence of the porous structure restricts the flow, and hence has a stabilizing influence.

The concept ofthe viscous potential flow is a fundamental topic in the theory of fluid mechanics. Joseph [11] attempted to identify the main events in the history throughout irrotational flow of viscous fluids. He showed that every theorem about potential flow of perfect fluids, with conservative body forces, applies equally in viscous fluids through regions of irrotational flow. The potential flow theory are not more difficult but have a much richer content when the viscous forces are incorporated only through the normal stress tensor condition. The irrotationalflows of viscous fluids are not good approximations for flows with distributed vorticity. In case of an incompressible flow, the velocity potential satisfies the Laplace's equation and potential theory is applicable. However, potential flows also have been used to describe compressible flows. The potential flow approach occurs in modeling of both stationary as well as non-stationary flows. Moatimid and Hassan [12] applied the viscous potential theory in the problem of electrohydrodynamic KHI through two porous media. They found that the Darcy's coefficients of the porous layers play a stabilizing role in the stability picture. Also, the existences of the injection velocities at both boundaries have stabilizing effect and vice-versa for the suction. Moatimid et al. [13] considered the viscous potential theory in a problem of nonlinear KHI through porous media. Their analysis may be considered as a generalization of the previous work of Moatimid and Hassan [12]. They found new stable and unstable regions in accordance to the influence of the nonlinear approach. Tiwari et al. [14] used the viscous potential flow theory to investigate a linear analysis of capillary instability of a cylindrical interface in the presence of an axial magnetic field with mass and heat transfer. They showed that axial magnetic field, as well as mass and heat transfer, hasa stabilizing effect on the system.Recently, Moatimid et al. [15] studied the stability of two cylindrical interfaces, where the fluids are saturated in porous media. Their analysis is carried out through a viscous potential flow theory. They showed that the porosity has a stabilizing picture and Darcy’s coefficient has a destabilizing influence.

Because of the great applications of electrohydrodynamic in various divers’ fields, the aim of this work is to study the electrohydrodynamic instability of double interfaces of a dielectric liquid sheet. Because of the instability in porous media may be of wide interest in geophysics and biomechanics, the current study is done through porous media. In accordance with the mathematical simplification of the viscous potential flow theory, the following analysis admits this concept. Therefore, we have extend previous work [2] to include all these aspects, i.e. to study the effect of porosity, Darcy's coefficient as well as kinematic viscosity on the stability of the problem at hand. General dispersion relation is obtained on using the normal modes analysis. The stability of the system is discussed both analytically and numerically. As we stated before, the periodic streaming of the same model will be considered in a subsequent paper. To clarify the problem, the plan of this work is outlined as follows: Section 2 is devoted to introduce the mathematical formulation of the problem and the corresponding

perturbation equations. The appropriate boundary-conditions are presented in Section 3. The formulation of the general dispersion equations is given in Section 4. From the point of view of the symmetric and anti-symmetric modes,a mathematical simplification of these equations is done. Also, differentspecial cases are reported in Section 5 and its subsections. Section 6 is devoted to introduce a numerical illustration of the general case. The concluding remarks are presented in Section 7.

2. Mathematical Formulation of the Problem and Perturbation Equations

An electrified liquid infinitely long horizontal liquid sheet of finite thickness 2a and embedded between two rigid boundaries of thicknesses $|h-a|$ is considered. Both fluids are uniform streaming, dielectric, viscous and incompressible. It is assumed that there are no volume charges through the three layers. In addition, no surface charges present at the interfaces. Without any less of generality, two-dimensional disturbances are only considered. For convenience, the Cartesian coordinates are used.

Figure 1 sketched the system under consideration, in the undisturbed state, where the $y-$axis is taken vertically upward and the $x-$axis is taken horizontally to be located at the center of the middle sheet. Generally, the subscripts *j* = 1, 2 and 3 refer to quantities in the upper, sheet and lower fluids, respectively. The system is influenced by the gravitational force (g) which acts in the negative y-direction. There are two undisturbed interfaces among the three fluids. They are assumed to be well defined and initially flat and form the planes $y=-a$ and $y=a$. All liquids are assumed to be of uniform nature, homogeneous and are all saturated in porous media. The structure of the liquids are defined from the following parameters; density ρ, dynamic viscosity μ, Darcy's coefficient ν, porosity ξ, uniform tangential electric field E_0 (which is constant along the three layers) and uniform stream V.

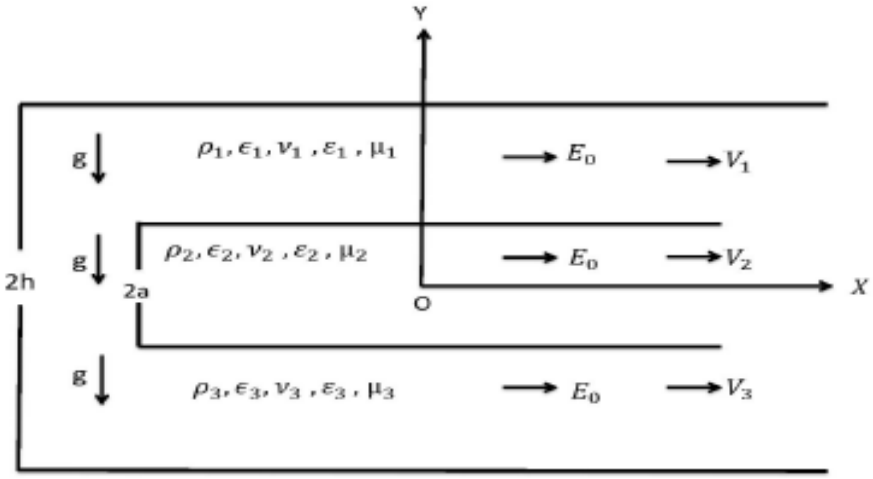

Figure 1: The system in the undisturbed state

The two interfaces are parallel and the flow in each phase is everywhere parallel to each other. After a small departure from the stationary state, the surface deflections may be expressed as follows:

In the light of the standard normal modes analysis [1], the surface deflections $\eta_j(x;t)$ may be given by a sinusoidal wave of finite amplitude where, after disturbance, the interface is represented by

$$y(x;t)=(-)^{j+1}a+\eta_j(x;t)\quad (j=1,2)\ , \tag{2.1}$$

and

$$\eta_j(x;t)=\gamma_j(t)e^{ikx}+c.c.\ , \tag{2.2}$$

where $\gamma_j(t)$ is an arbitrary time-dependent function, which determines the behavior of the amplitude of the disturbance at the interface, k is the wave number which is assumed to be real and positive and c.c. represents the complex conjugate of the proceeding term.

It is convenient to determine aunit outward normal vector to the interfaces. This is may be obtaining from the relation $n_j = \nabla S_j / |\nabla S_j|$, where $S_j(x,y;t)$ is the surface's geometry which is defined by $S_j = y - (-)^{j-1} a - \eta_j(x;t).$

Therefore,

$$\hat{n}_j = -(\partial \eta_j / \partial x)\underline{e}_x + \underline{e}_y, \tag{2.3}$$

where $\underline{e}_x$ and $\underline{e}_y$ are the unit vectors along the $x-$and $y-$directions, respectively.

As a result of a perturbation, the initial fluid velocity increases and permits to introduce a scalar potential $\phi(x,y;t)$, such that

$$\underline{v}_j = V_j\ \underline{e}_x + \nabla\phi_j, \quad (j = 1,2,3) \tag{2.4}$$

Since the three fluids layers are incompressible, the scalar potential $\phi(x,y;t)$ is being a harmonic function, i.e.

$$\nabla^2\phi_j = 0, \ (j = 1,2,3) \tag{2.5}$$

The equation that governs the behavior of the fluid through porous media according to the Brinkman-Darcy equation is given by

$$\frac{\rho_j}{\xi_j}\left(\frac{\partial \underline{v}_j}{\partial t} + \frac{1}{\xi_j}(\underline{v}_j.\nabla)\underline{v}_j\right) = -\nabla P_j - \upsilon_j \underline{v}_j - \rho_j\, g\, \underline{e}_y, \tag{2.6}$$

where ξ_j represents the porosity of the medium. The frictional forces resulted from the interactive force between the fluid and the porous medium. Itis proportional to the flow velocity which represents by the term $\upsilon_j \underline{v}_j$, where $\upsilon_j = (\mu_j / q_j)$is the Darcy's coefficient, μ_j is the fluid viscosity and q_j is the permeability of the porous medium.

In accordance with the viscous potential flow theory, the viscous fluid may be considered as an irrotational liquid and then obeys the Laplace equation.

A number of simplifications of the Maxwell's equations [16] are appropriate to the description of electrodynamics' phenomena for the fluid system. The electrical Maxwell's equations are reduced to:

$$\nabla.(\varepsilon_j \underline{E}_j) = 0, \quad (j = 1,2,3) \tag{2.7}$$

and

$$\nabla \times \underline{E}_j = 0. \tag{2.8}$$

Therefore, the electric field may be written as:

$$E_j = E_0\ \underline{e}_x - \nabla\psi_j, \tag{2.9}$$

where $\psi_j(x,y;t)$ is an electrostatic potential. The amplitude of the surface waves, formed on the fluid sheet, is assumed to be small. Combining equations (2.7) and (2.9), one gets

$$\nabla^2\psi_j = 0, \quad (j = 1,2,3) \tag{2.10}$$

For a small disturbance from the equilibrium state, the electrostatic potential and the velocity potential can be written in the form

$$\psi_j(x,y;t) = \hat{\psi}_j(y;t)\, e^{ikx} + c.c, \quad (j = 1,2,3) \tag{2.11}$$

and

$$\phi_j(x,y;t)=\hat{\phi}_j(y;t)\ e^{ikx}+c.c, \tag{2.12}$$

The solutions of the linearized equations (2.5) and (2.10) give

$$\phi_j(x,y;t)=\left[A_j(t)\cosh(ky)+B_j(t)\sinh(ky)\right]e^{ikx}+c.c, \tag{2.13}$$

and

$$\psi_j(x,y;t)=\left[C_j(t)\cosh(ky)+D_j(t)\sinh(ky)\right]e^{ikx}+c.c, \tag{2.14}$$

where $A_j(t),\ B_j(t), C_j(t)$ and $D_j(t)$ are arbitrary functions of time which are to be determined by making use of the appropriate boundary conditions.

3. Boundary Conditions

To complete the formulation of the problem at hand, the general solutions of the potentials ϕ_j and ψ_j as given in equations (2.13) and (2.14) must be completely determined. This requires evaluating the arbitrary time dependent functions that appearing in these equations. Therefore, for the purpose of specifying these unknown functions, it convenient to identify two types of boundaries. The first is that at the surface between a fluid and a rigid surface. The second is at the fluid / fluid interfaces. Therefore, the boundary conditions may be formulated as follows:

3.1. At the Rigid Boundaries

(I) The normal fluid velocities must be vanished at the bottom and top boundaries, this requires

$$\frac{\partial\phi_1}{\partial y}=0 \qquad \text{at} \qquad y=h, \tag{3.1}$$

and

$$\frac{\partial\phi_3}{\partial y}=0 \qquad \text{at} \qquad y=-h, \tag{3.2}$$

(II) The tangential components of the electric field must be vanished at these boundaries, these yields

$$\frac{\partial\psi_1}{\partial x}=0 \qquad \text{at} \qquad y=h, \tag{3.3}$$

and

$$\frac{\partial\psi_3}{\partial x}=0 \qquad \text{at} \qquad y=-h, \tag{3.4}$$

3.2. At the Fluid/Fluid Interfaces

(I) The kinematic relation follows from the assumption that the normal component of the velocity vector in each phases of the system is continuous at the dividing surfaces. This implies that

$$\underline{v}_{n_j}=\frac{dS_1}{dt}=0 \text{ for } y=a+\eta_1, \quad (j=1,2), \tag{3.5}$$

and

$$\underline{v}_{n_j}=\frac{dS_2}{dt}=0 \text{ for } y=-a+\eta_2, \quad (j=2,3), \tag{3.6}$$

where the material derivative is defined as: $\frac{d}{dt}=\frac{\partial}{\partial t}+(\bar{v}.\nabla).$

Maxwell's conditions for the electric potential:

The Maxwell's conditions for an electric potential, where there are no surface charges presenting at the interfaces. Also, there are no volume charges are assumed to present in the bulk of the three fluid layers.

(II) The jump, in the tangential component of the electric field is equal zero across the interfaces:

$$\underline{n}_j \times \left\| \underline{E}_j \right\| = 0, \text{ at } \quad y(x;t) = (-)^{j+1} a + \eta_j(x;t), \quad (j = 1,\ 2), \tag{3.7}$$

where $\| \ \|$ represents the difference (jump) in a quantity as we cross the interface, i.e, $\|f\| = f_1 - f_2$, where the subscripts refer to two different media.

In other words:

$$\frac{\partial \psi_1}{\partial x} = \frac{\partial \psi_2}{\partial x} \qquad \text{at} \qquad y = a + \eta_1, \tag{3.8}$$

and

$$\frac{\partial \psi_2}{\partial x} = \frac{\partial \psi_3}{\partial x} \qquad \text{at} \qquad y = -a + \eta_2, \tag{3.9}$$

(III) The continuity of normal component of the electric displacement at the surface of separation, requires

$$\underline{n}_1 . \left(\varepsilon_1 \underline{E}_1 - \varepsilon_2 \underline{E}_2 \right) = 0, \qquad (j = 1,2) \text{ for} \qquad y = a + \eta_1, \tag{3.10}$$

and

$$\underline{n}_2 . \left(\varepsilon_2 \underline{E}_2 - \varepsilon_3 \underline{E}_3 \right) = 0, \qquad (j = 2,3) \text{ for} \qquad y = -a + \eta_2, \tag{3.11}$$

Applying the forgoing boundary conditions on the general solution (2.13), (2.14), one gets the following:

For the hydrodynamic part:

$$\phi_1(x,y;t) = \frac{\cosh[k(h-y)]}{k \sinh[k(h-a)]} \left(\gamma_1'(t) + i k V_1 \gamma_1(t) \right) e^{ikx}, \tag{3.12}$$

$$\phi_2(x,y;t) = \frac{1}{k \sinh[2ak]} \left(\cosh[k(a-y)](\gamma_2'(t) + i k V_2 \gamma_2(t)) - \cosh[k(a+y)](\gamma_1'(t) + i k V_2 \gamma_1(t)) \right) e^{ikx}, \tag{3.13}$$

and

$$\phi_3(x,y;t) = \frac{-\cosh[k(h+y)]}{k \sinh[k(h-a)]} \left(\gamma_2'(t) + i k V_3 \gamma_2(t) \right) e^{ikx}. \tag{3.14}$$

For the electric part:

$$\begin{aligned} \psi_1(x,y;t) = \frac{i}{\varepsilon^*} e^{ikx} \sinh[k(h-y)] E_0 (2\varepsilon_2(\varepsilon_2 - \varepsilon_3)\sinh[k(a-h)]\gamma_2(t) + \\ ((\varepsilon_2 - \varepsilon_3)\sinh[k(3a-h)] - (\varepsilon_2 + \varepsilon_3)\sinh[k(a+h)])(\varepsilon_1 - \varepsilon_2)\gamma_1(t)), \end{aligned} \tag{3.15}$$

$$\begin{aligned} \psi_2(x,y;t) = \frac{i}{\varepsilon^*} e^{ikx} \sinh[k(a-h)] E_0 (((-\varepsilon_2 + \varepsilon_3)\sinh[k(2a-h+y)] + \\ (\varepsilon_2 + \varepsilon_3)\sinh[k(h+y)])\ (\varepsilon_1 - \varepsilon_2)\gamma_1(t) + ((\varepsilon_1 - \varepsilon_2)\sinh[k(2a-h-y)] + \\ (\varepsilon_1 + \varepsilon_2)\sinh[k(h-y)])\ (\varepsilon_2 - \varepsilon_3)\gamma_2(t)), \end{aligned} \tag{3.16}$$

And

$$\begin{aligned} \psi_3(x,y;t) = \frac{i}{\varepsilon^*} e^{ikx} \sinh[k(h+y)] E_0 (2\varepsilon_2(\varepsilon_1 - \varepsilon_2)\sinh[k(a-h)]\gamma_1(t) + \\ ((-\varepsilon_1 + \varepsilon_3)\sinh[k(3a-h)] - (\varepsilon_1 + \varepsilon_2)\sinh[k(a+h)])\ (\varepsilon_2 - \varepsilon_3)\gamma_1(t)), \end{aligned} \tag{3.17}$$

where ε^* is given by

$$\begin{aligned} \varepsilon^* = \varepsilon_2(\varepsilon_1 + \varepsilon_3)\cosh(2ak)\sinh[2k(a-h)] + (\varepsilon_2^2 - \varepsilon_1\varepsilon_3)\sinh(2ak) - \\ (\varepsilon_2^2 + \varepsilon_1\varepsilon_3)\cosh[2k(a-h)]\sinh(2ak). \end{aligned} \tag{3.18}$$

As a result of perturbation, the pressure may be written as:

$$P_j = P_0^{(j)} + P_1^{(j)}, \tag{3.19}$$

where

$$P_0^{(j)} = -\upsilon_j V_j\, x - \rho_j\, g\, y + \lambda_j, \tag{3.20}$$

where λ_j is an arbitrary time-dependent function.

From the continuity of the normal stresses in the zero-order at the interface, one gets

$$\lambda_j - \lambda_{j+1} = (-)^{j+1}(\rho_j - \rho_{j+1})\, g\, a + (\upsilon_j V_j - \upsilon_{j+1} V_{j+1})x + \frac{1}{2}(\varepsilon_j - \varepsilon_{j+1})\, E_0^2,\ (j = 1,2). \tag{3.21}$$

The pressure in the first-order of may be evaluated from the Bernoulli's equation. In other words, the integration of the equation of motion (2.6) yields

$$P_1^{(j)}(x, y; t) = \frac{\rho_j}{\xi_j}\frac{\partial \phi_j}{\partial t} + \frac{\rho_j V_j}{\xi_j^2}\frac{\partial \phi_j}{\partial x} + \upsilon_j \phi_j, \quad (j = 1,2,3) \tag{3.22}$$

Substituting from equations (3.12), (3.13) and (3.14) into Eq. (3.22), one find

$$P_1^{(1)} = \frac{\cosh[k(h-y)]}{k\,\xi_1^2 \sinh[k(a-h)]} e^{ikx}\left[k^2 V_1^2 \rho_1 \gamma_1(t) - \xi_1(\upsilon_1 \xi_1 \gamma_1'(t) + \rho_1 \gamma_1''(t)) - ikV_1\left(\upsilon_1 \xi_1^2 \gamma_1(t) + (1+\xi_1)\rho_1 \gamma_1'(t)\right)\right], \tag{3.23}$$

$$P_2^{(1)} = \frac{1}{k\,\xi_2^2 \sinh(2ak)} e^{ikx}[\cosh[k(a+y)](k^2 V_2^2 \rho_2 \gamma_1(t) - \xi_2\left(\upsilon_2 \xi_2 \gamma_1'(t) + \rho_2 \gamma_1''(t)\right) - ikV_2(\upsilon_2 \xi_2^2 \gamma_1(t) + (1+\xi_2)\rho_2 \gamma_1'(t))) - \cosh[k(a-y)](k^2 V_2^2 \rho_2 \gamma_2(t) - \xi_2\left(\upsilon_2 \xi_2 \gamma_2'(t) + \rho_2 \gamma_2''(t)\right) - ikV_2(\upsilon_2 \xi_2^2 \gamma_2(t) + (1+\xi_2)\rho_2 \gamma_2'(t))], \tag{3.24}$$

and

$$P_3^{(1)} = \frac{-\cosh[k(h+y)]}{k\,\xi_3^2 \sinh[k(a-h)]} e^{ikx}\left[k^2 V_3^2 \rho_3 \gamma_2(t) - \xi_3\left(\upsilon_3 \xi_3 \gamma_2'(t) + \rho_3 \gamma_2''(t)\right) - ikV_3\left(\upsilon_3 \xi_3^2 \gamma_2(t) + (1+\xi_3)\rho_3 \gamma_2'(t)\right)\right], \tag{3.25}$$

The remaining boundary condition may be formulated as follows:

In accordance with the viscous potential flow, the viscous terms will enter only through the normal stress balance. As stated before, it is ignored throughout the linear conservation of momentum. Therefore, the influence of the electric field and viscosity are considered only, in the normal stress tensor balance at the interface, at which the viscosity forces are neglected elsewhere. In order to complete the linear stability analysis, the remaining boundary condition arises from the normal component of the total stress tensor. This component is discontinuous at the interface by the amount of the surface tension.

The total stress tensor of the system under investigation is defined as,

$$\sigma_{ij} = \sigma_{ij}^{vis} + \sigma_{ij}^{mag}, \tag{3.26}$$

where, σ_{ij}^{vis} is the viscous stress tensor and σ_{ij}^{mag} is the Maxwell magnetic stress.

These stresses may be formulated as follows:

(i) The Viscous Stress Tensor

A large number of practically important fluids (e.g. water and oil) are incompressible and exhibit a linear relation between the shear rate and strain. These fluids are well-known as the Newtonian fluids and their constitutive equation is given by

$$\sigma_{ij}^{vis} = -P\delta_{ij} + \mu\left(\frac{\partial v_i}{\partial x_j} + \frac{\partial v_j}{\partial x_i}\right), \tag{3.27}$$

where P is the pressure in the fluid and δ_{ij} is the Kronecker's delta.

It is worthwhile to note that, there are also many fluids which do not behave as the Newtonian fluids and have different constitutive equations e.g. toothpaste. Not imaginatively, these one of ten called non-Newtonian fluids.

(ii) Maxwell Electric Stress

The electrostatics and hydrodynamics are coupled together through the Maxwell stress tensor. In vacuum, the Coulomb force density exerted on free charges may be rearranged noting the solenoid nature of the electrostatic field. The derivation of the Maxwell stress tensor for a dielectric medium is given in details by Melcher [16], Panofsky and Phillips [17], to obtain

$$\sigma_{ij}^{ele} = \varepsilon E_i E_j - \frac{1}{2}\varepsilon E_i^2 \delta_{ij}. \tag{3.28}$$

4. Derivation of the Dispersion Equation

The components of the total force per unit area, exerted on the fluid interface are related to components of the stress tensor, via the following relation:

$$\underline{F} = \begin{pmatrix} \sigma_{xx} & \sigma_{xy} \\ \sigma_{yx} & \sigma_{yy} \end{pmatrix} \begin{pmatrix} n_x \\ n_y \end{pmatrix}. \tag{4.1}$$

At the fluid interfaces, the normal component of the stress tensor is discontinuous by the amount of the surface tension. This requires

$$n \cdot \|F\| = T_{j(j+1)} \nabla^2 \underline{S}_j, \quad (j = 1,2) \tag{4.2}$$

where $T_{j(j+1)}$ is the surface tension coefficient of the surfaces separating fluid (j) from fluid (j + 1). Substituting from the solutions of $\phi_1^{(j)}, \psi_1^{(j)}$ and $P_1^{(j)}$ into the normal stress condition (4.2), after lengthy butstraightforward calculations, one obtains the following coupled equations:

$$\begin{aligned} &f_{11}\gamma_1''(t) + f_{22}\gamma_2''(t) + (l_{11} + ig_{11})\gamma_1'(t) + (l_{22} + ig_{22})\gamma_2'(t) + \\ &(a_{11} + E_0^2 b_{11} + i c_{11})\gamma_1(t) + (a_{22} + E_0^2 b_{22} + i c_{22})\gamma_2(t) = 0, \end{aligned} \tag{4.3}$$

and

$$\begin{aligned} &f_{22}\gamma_1''(t) + f_{12}\gamma_2''(t) + (l_{21} + ig_{22})\gamma_1'(t) + (l_{12} + ig_{12})\gamma_2'(t) + \\ &(a_{21} + E_0^2 b_{21} + i c_{21})\gamma_1(t) + (a_{12} + E_0^2 b_{12} + i c_{12})\gamma_2(t) = 0, \end{aligned} \tag{4.4}$$

where the coefficients f_{ij}, l_{ij}, g_{ij}, a_{ij}, b_{ij}, and c_{ij} are given in the Appendix.

Similar equations, in case of immiscible fluids, are early obtained by Moatimid [2].

Now, the boundary-value problem has been completed. The elevation amplitudes γ_1 and γ_2, as functions of time, determine the eigen-value functions. The nature of these functions governs the stability behavior of the fluid sheet. For simplicity, the present study is done through the symmetric and anti-symmetric modes as given in the following subsection.

4.1.The Symmetric and Anti-symmetric Analysis

The coupled differential equations (4.3) and (4.4) can be simplified by considering the symmetric and anti-symmetric deformations of the surface deflections η_1 and η_2. Therefore, the variables η_1 and η_2 may be described by

$$\eta_2 = J\eta_1 = \eta, \tag{4.5}$$

where $J = 1$ defines to the anti-symmetric deformation, while $J = -1$ refers to the symmetric one.

Considering the transformation (4.5) in the characteristic equations (4.3) and (4.4), one gets

$$(f_{11}+J\,f_{22})\gamma''(t)+\big((l_{11}+J\,l_{22})+i\,(g_{11}+J\,g_{22})\big)\gamma'(t)+$$
$$\big((a_{11}+J\,a_{22})+E_0^2\,(b_{11}+J\,b_{22})+i\,(c_{11}+J\,c_{22})\big)\gamma(t)=0, \tag{4.6}$$

and

$$(f_{22}+J\,f_{12})\gamma''(t)+\big((l_{21}+J\,l_{12})+i\,(g_{22}+J\,g_{12})\big)\gamma'(t)+$$
$$\big((a_{21}+Ja_{12})+E_0^2\,(b_{21}+J\,b_{12})+i\,(c_{21}+J\,c_{12})\big)\gamma()t)=0, \tag{4.7}$$

The coupled differential equations (4.6) and (4.7) may be combined by adding them to give a single dispersion equation as

$$\gamma''(t)+\big(L_1+iG_1\big)\gamma'(t)+\big(L_2+iG_2\big)\gamma\ (t)=0, \tag{4.8}$$

where the coefficients in Eq. (4.8) are well-known from the context. To avoid the lengthy of the paper, they will be omitted.

Equation (4.8) is a linear homogeneous differential equation with constant complex coefficients. Therefore, the exponential solution is valid. Therefore, the solution of the dispersion equation (4.9), may be written as

$$\gamma(t)=\delta\,e^{-i\,\omega t}, \tag{4.9}$$

where δ is a real constant parameter, and ω is a complex constant which determines the natural frequency of the surface wave. From equations (4.8) and (4.9), one finds

$$\omega^2+Q_1\omega+Q_2=0, \tag{4.10}$$

where $Q_1=-G_1+i\,L_1$ and $Q_2=-(L_2+iG_2)$..

Equation (4.10) represents a linear dispersion relation with complex coefficients for the double surface waves that propagate through the magnified streaming sheet in porous media. This dispersion relation is satisfied by the values of ω and k. Therefore, if the imaginary part of ω is positive, the disturbance will temporally grow with time and the flow will unstable. On the other words, if the imaginary part of ω is negative, the disturbances will decay with time and the flow becomes stable.

It is well-known from the Routh-Hurwitz criterion [18], that the necessary and sufficient stability conditions for (4.10) are

$$\mathrm{Re}(Q_1)>0, \tag{4.11}$$

and

$$\mathrm{Re}(Q_1)\,\mathrm{Re}(Q_1\overline{Q}_2)-(\mathrm{Im}Q_2)^2>0. \tag{4.12}$$

At this stage, the linear stability analysis has been theoretically completed. To complete the stability picture, numerical discussions are needed. Before going to the general case, some special cases are reported upon appropriate data choices.

5. Special Cases

It is more convenient to discuss the stability analysis for some special case in detail. These cases may be formulated as follows:

5.1 For an Inviscid, non-Porous, and non-Streaming Fluid

At this case, considering the limits, where $\mu_j=0, V_j=0, \upsilon_j=0$ and $\xi_j=1$ for ($j=1,2,3$). In this case the dispersion relation (4.10) is reduced to the following simplest form

$$\omega^2-R_1=0, \tag{5.1}$$

where R_1 is well-known from the context. To avoid the lengthy of the paper, they will be omitted.

Therefore, the interfaces between the fluids are stable or unstable according whether ω is real or complex. Since our aim is to study amplitude modulation of the progressive waves, we assume that $\omega^2>0$.

Therefore, the system is linearly stable if

$$\alpha_1 E_0^2 + \beta_1 > 0, \tag{5.2}$$

where α_1 and β_1 arewell-known from the context. To avoid the lengthy of the paper, they will be omitted.

The influence of the electric field on the stability depends mainly on the sign of the parameter α_1. If $\alpha_1 > 0$ it follows that E_0^2 has a stabilizing influence and vice-verse when $\alpha_1 < 0$.

Before dealing with a numerical calculation, it is convenient to write the stability criterion in an appropriate dimensionless form. This can be done in a number of ways depending primarily on the choice of the characteristic length. Consider the dimensionless forms depending on the characteristic length $= h$, the characteristic time $= \sqrt{h/g}$ and the characteristic mass $= hT_{23}/g$, the other dimensionless quantities are given by

$k = k^*/h, a = a^* h,\ \rho_j = \rho_j^* T_{23}/gh^2,\ T_{12} = T_{12}^* T_{23}$, and $E_0^2 = (E_0^*)^2 T_{23}/h \quad (j = 1,2,3)$.

From now on, for simplicity, the " * " mark may be dropped.

Generally, our interest is focused on the relation between the electric field intensity $Log(E_0^2)$ and the wave number of the surface waves k. Therefore, the stability diagram is plotted for $Log(E_0^2)$ versus k. In the following figures, the stable region is characterized by the latter S. Meanwhile, the latter U stands for the unstable one.

In what follows, a numerical calculation is performed for a given special case. These figures considered, only, the symmetric case. Through Fig.2, the influence of sheet thickness (a) is depicted. Therefore, $Log(E_0^2)$ is plotted versus the wave number k according to different values of (a). The calculations show that the parameter α_1 is always positive during the given domain of the dependent function. This means a stabilizing influence of the tangential electric field. Actually, it is an early sense. This figure shows that the stability of the system is enhanced with the increasing of the parameter (a), especially, at large values of the wave number k. Therefore, the layer thickness (a) plays a stabilizing influence in the stability picture. Fig.3 is plotted to indicate the influence of the dielectric parameter ε_2 in the stability picture. It is shown that ε_2 has a stabilizing influence especially at large value of the wave number k.

5.2. For Viscous, non-Porous, and non-Streaming Fluid

Now, considering alimiting case, where $V_j = 0, \upsilon_j = 0$ and $\xi_j = 1$ for $(j = 1,2,3)$. In this case the dispersion relation (4.8) is reduced to the following simplest form:

$$\gamma''(t) + R_2\gamma'(t) + R_1\gamma(t) = 0. \tag{5.3}$$

Let $\gamma(t) = f(t)e^{-R_2 t/2}$ after substituting in Eq. (5.3), one finds

$$f''(t) + (R_1 - \frac{1}{4}R_2^2) f(t) = 0, \tag{5.4}$$

assuming that $f(t) = f_0 e^{i\theta t}$ where f_0 is real constant, one gets

$$\theta^2 - (R_1 - \frac{1}{4}R_2^2) = 0. \tag{5.5}$$

It follows that the stability requires

$$(R_1 - \frac{1}{4}R_2^2) > 0, \tag{5.6}$$

or

$$\alpha_1 E_0^2 + \beta_2 > 0, \tag{5.7}$$

where R_2 and β_2 are well-known from the context. To avoid the lengthy of the paper, they will be omitted.

It is clear that R_2 is independent on the electric field intensity E_0^2, but the condition of positive R_2 is necessary for the stability requirements. Therefore, the domain in the figure $Log(E_0^2) - k$ must be consistent with the positivity of R_2.

At this end, consider the following dimensionless forms: the characteristic length $= h$, the characteristic time $= \sqrt{h/g}$ and the characteristic mass $= \mu_2 h\sqrt{h/g}$.

The theoretical analysis includes two modes of surface deformations. Therefore, Fig.4 and Fig.5 are plotted to indicate the influence of the dynamic viscosity μ_1, through the symmetric and anti-symmetric. It is shown in Fig.4 (J = 1) that the parameter μ_1 has a destabilizing influence. This influence is enhanced at large values of k. In contrast with the previous mode, Fig.5 is graphed with the case of a symmetric mode (J = −1) for the variation of the same parameter μ_1. In this sense, the parameter μ_1 plays a dual role in the stability criterion according to the different modes. Through Fig.6, the influence of the sheet thickness (a) is depicted. It is shown that the sheet thickness has a stabilizing influence.

5.3. For Viscous, Porous, and non-Streaming Fluid

In this case, the streaming velocities are ignored. It follows that the general dispersion equation (4.8), may be written as:

$$\gamma''(t) + R_3\gamma'(t) + R_4\gamma(t) = 0. \tag{5.8}$$

The normal form of Eq. (5.8) may be obtained according to the transformation $\gamma(t) = f(t)e^{-R_3 t/2}$.

Therefore, the arbitrary function $f(t)$ should satisfy the following equation:

$$f''(t) + (R_4 - \frac{1}{4}R_3^2) f(t) = 0, \tag{5.9}$$

assuming that $f(t) = f_0 e^{i\theta t}$ where f_0 is real constant, one finds

$$\theta^2 - (R_4 - \frac{1}{4}R_3^2) = 0. \tag{5.10}$$

The system is linear stable if θ^2 is positive, $(R_4 - \frac{1}{4}R_3^2)$ can be written in the form

$$\alpha_2 E_0^2 + \beta_3 > 0, \tag{5.11}$$

where R_3, R_4, α_2 and β_3 are well-known from the context. To avoid the lengthy of the paper, they will be omitted.

The calculations showed that R_3 is independent on the electric field intensity E_0^2, but the condition on R_3 is necessary for the stability requirements. Therefore, the domain in the figure $Log(E_0^2) - k$ must be consistent with the positivity of R_3.

The following figures are deal with the symmetric mode only. The influence of the parameter ξ_1 is depicted in Fig. 7. It is shown that variation of this parameter has a stabilizing role, especially, at large values of the wave number k. The effect of the dynamic viscosity μ_1 is depicted in Fig.8. It is shown the increasing of this parameter has a destabilizing role in the stability picture.

6. Numerical Discussion for the General Case

Eq. (4.10) is an algebraic quadratic equation with complex coefficient. As stated above, the stability criteria depend mainly in the nature of the frequency ω. According to the Routh-Hurwitz criteria [18], the necessary and sufficient stability conditions for (4.11), (4.12) may be formulated as

$$G_1 < 0, \tag{6.1}$$

and $\alpha\ E_0^2 + \beta < 0$, (6.2)

where α and β are well-known from the context. To avoid the lengthy of the paper, they will be omitted.

We used the same dimensionless quantities as given in Section (5.2).

In what follows, a numerical calculation, for the anti-symmetric case, is performed for the general case. As stated before, the implication of the condition (6.1) must be taken into account. The following figures are plotted for a domain of the wave number such that this condition (6.1) is automatically satisfied. In addition, all the present calculations indicate that the parameter α is always has a negative sign. This shows again that the electric field intensity has a stabilizing influence, which is an early fact, proved by many researches.

Through Fig.9, the influence of Darcy's coefficient of fluid (υ_2) is depicted. It is shown that the Darcy's coefficient has a destabilizing influence. Fig. 10 shows an important influence of the dynamic fluid viscosity and its effect on stability of system. The dynamic fluid viscosity has a destabilizing effect, especially, at large values of wave number k. In Fig. 11, the influence of the uniform streaming (V_2) is depicted. The uniform streaming has a destabilizing influence. This role is enhanced as the relative motion between the two fluid layers is increased. This result is in agreements with different studies in the linear stability theory, for example (Chandrasekhar [1]). Fig.12 displays the natural stability curve for various values of the sheet thickness (a). As shown in this figure, the stability is increased at small values of the wave number. Meanwhile, at large values of the wave number, the instability in enhanced. This shows the dual role of the sheet thickness in the stability picture. Through Fig.13, it is shown that the influence of fluid porosity (ξ_2) is depicted. The porosity has also a dual role effect.

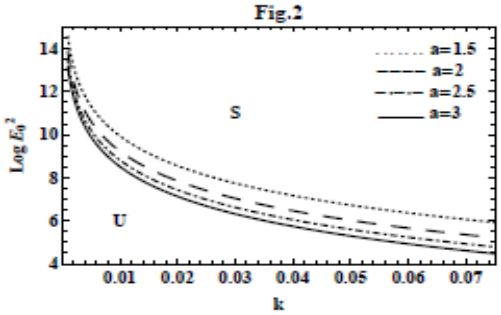

Figure 2: Plots a stability diagram, according to the condition (5.2) for a system having the particulars:

$\rho_1 = 2, \rho_2 = 4, \rho_3 = 6, J = 1, \varepsilon_1 = 3, \varepsilon_2 = 5, \varepsilon_3 = 10$ *and* $T_{12} = 15$.

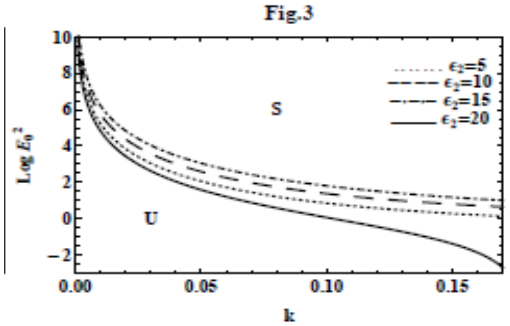

Figure 3: Plots a stability diagram, according to the condition (5.2) for a system having the particulars:

$\rho_1 = 0.001, \rho_2 = 0.01, \rho_3 = 1, J = 1, \varepsilon_1 = 30, \varepsilon_3 = 10, a = 3$ *and* $T_{12} = 25$.

Fig.4

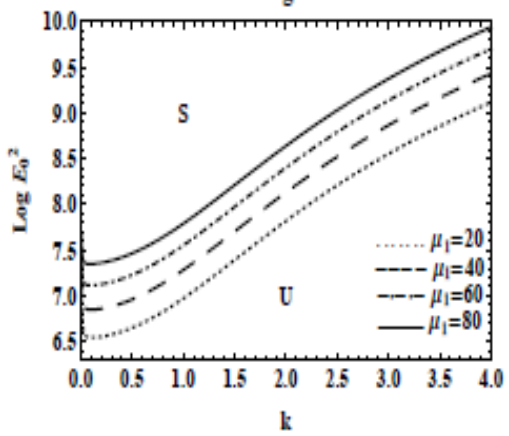

Figure 4: Plots a stability diagram, according to the condition (5.7) for a system having the particulars: $\rho_1 = 0.001, \rho_2 = 0.01, \rho_3 = 1, J = 1, \varepsilon_1 = 25, \varepsilon_2 = 5, \varepsilon_3 = 10, \mu_3 = 100, T_{23} = 15, a = 2$ *and* $T_{12} = 25$.

Fig.5

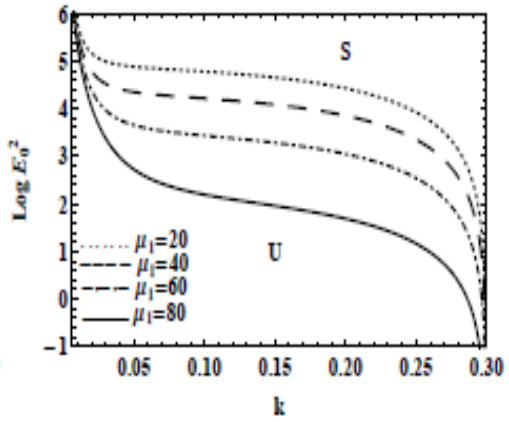

Figure 5: Stability diagram for the same system as consider Fig.4 except $J = -1, \varepsilon_1 = 5, \varepsilon_2 = 50$ *and for various values of* μ_1.

Fig.6

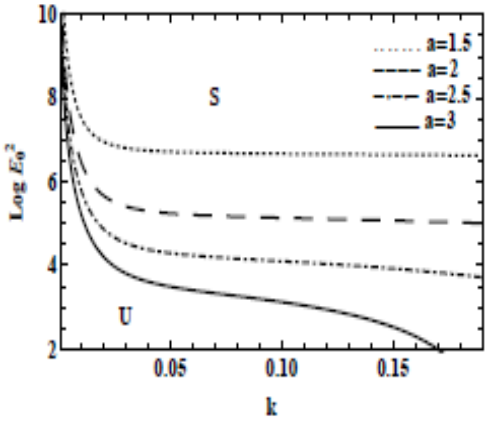

Figure 6: Stability diagram for the same system as consider Fig.4 except $\varepsilon_1 = 35, \varepsilon_2 = 20, \mu_1 = 10, \mu_3 = 50$ *and for the various value of* a.

Fig.7

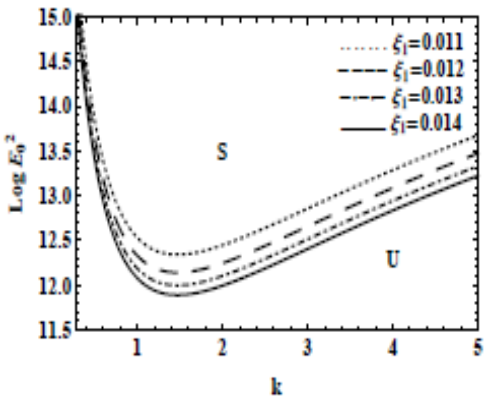

Figure 7: Plots a stability diagram, according to the condition (5.11) for a system having the particulars:

$a=0.5, \rho_1=0.001, \rho_2=0.01, \rho_3=0.1, J=-1, \varepsilon_1=4.6,\ \varepsilon_2=6,\ \varepsilon_3=3, \xi_2=0.3, \xi_3=0.8,$
$\mu_1=50, \mu_3=20, \upsilon_1=100, \upsilon_2=80, \upsilon_3=60, T_{23}=50$ *and* $T_{12}=30$.

Fig.8

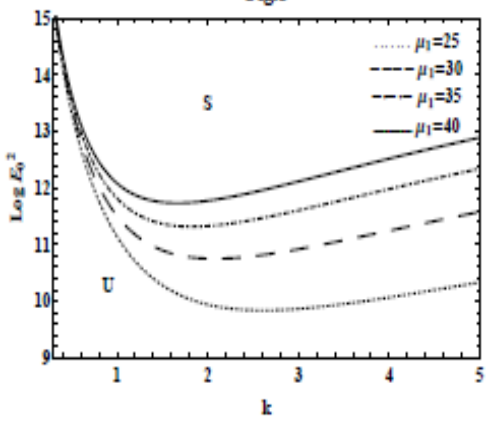

Figure 8: Plots a stability diagram, according to the condition (5.11) for a system having the particulars:

$a=2, \rho_1=1.25, \rho_2=3.25, \rho_3=5.75, J=-1, \varepsilon_1=0.3,\ \varepsilon_2=5.10,\ \varepsilon_3=1.5, \xi_1=0.15,\ \xi_2=0.03,$
$\xi_3=0.3, \mu_3=500, \upsilon_1=10, \upsilon_2=50, \upsilon_3=50, V_1=5, V_2=10, V_3=8, T_{23}=15$ *and* $T_{12}=45$.

Fig.9

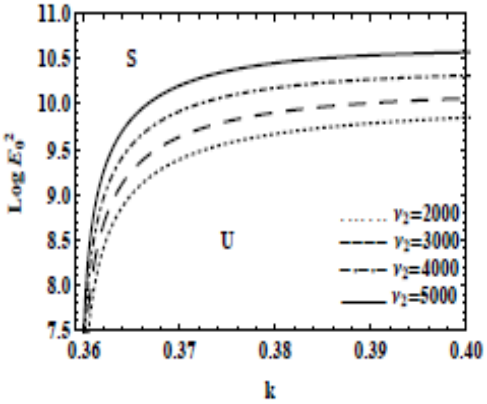

Figure 9: Plots a stability diagram, according to the condition (6.2) for the system as consider Fig.8 except $\mu_1=100, V_2=2$ *and for various values of* υ_2.

Fig.10

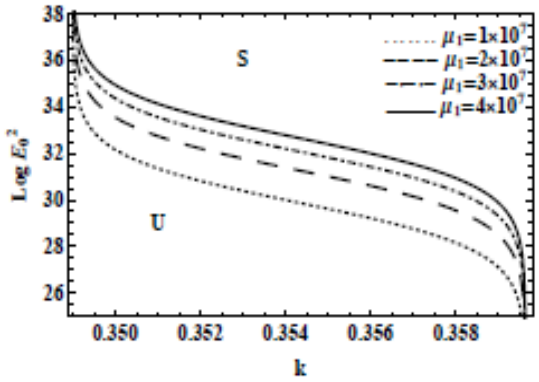

Figure 10: Plots a stability diagram, according to the condition (6.2) for the system as consider Fig.8except $\upsilon_1 = 100, \upsilon_2 = 200, \upsilon_3 = 300,\ V_1 = -5, V_2 = 2, V_3 = 0.5, T_{23} = 5,\ T_{12} = 15$ *and for various values of* μ_1 .

Fig.11

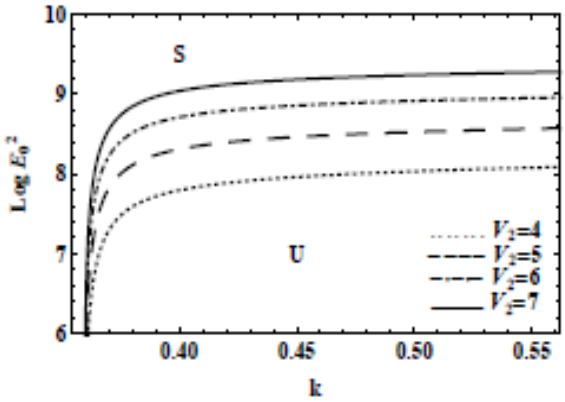

Figure 11: Stability diagram for the same system as consider Fig.10 except $\mu_3 = 5, \upsilon_1 = 20, \upsilon_2 = 40$ *and for various values of* V_2 .

Fig.12

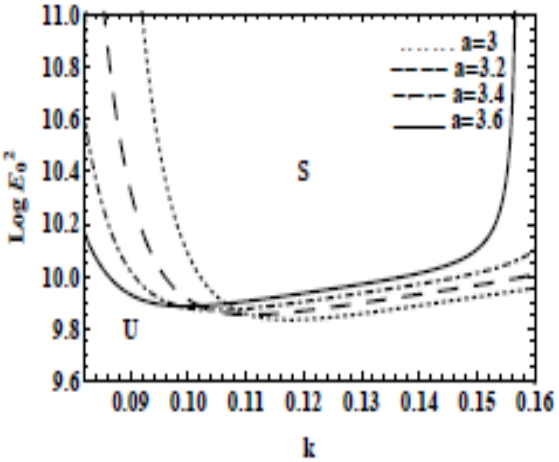

Figure 12: Plots a stability diagram, according to the condition (6.2) for the system as consider Fig.8 except $\mu_1 = 10, \mu_3 = 25, \upsilon_1 = 30, \upsilon_2 = 5,\ \upsilon_3 = 15,$ *and for the various value of* a.

Fig.13

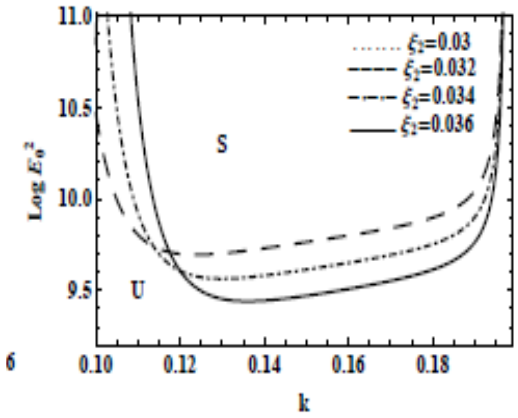

Figure 13: Stability diagram for the same system as consider Fig.12 except $a = 2$ *and for various values of* ξ_2

7. Concluding Remarks

In the present paper, we have formulated a problem of electrohydrodynamic KHI of a horizontal liquid dielectric sheet of finite thickness and embedded between two finite layers. The liquids are saturated in porous media, where the porosity of the media is taken into account. In accordance with the wide applications of the viscous fluids, the viscosity is, also, considered. To relax the manipulation of the analysis, the viscous potential flow theory is adapted. Therefore, the viscous effects are demonstrated only, through the normal stress tensor condition. The analysis is based on the normal modes technique to achieve the linear stability analysis. The boundary value problem leads to coupled simultaneous ordinary differential equations with damped and complex coefficients. The analysis includes only the symmetric as well as anti-symmetric modes. Several special cases are recovered upon appropriate data choices. The influence of the periodic streaming will be investigated in a subsequent paper. The general case considered only the anti-symmetric mode. The stability and instability of the system are addressed through a set of diagrams.

References

[1]. S. Chandrasekhar, Hydrodynamic and Hydromagnetic Stability, Clarendon Press, Oxford (1961).
[2]. G. M. Moatimid, Stability conditions of an electrified miscible viscous fluid sheet, Journal of Colloid and Interface Science, 259(1), 186-199 (2003).
[3]. E. F. El-Shehawey, Y. O. El-Dib, and A. A. Mohamed, Electrohydrodynamic stability of a fluid layer, Effect of a tangential field, IL Nouvo Cimento, 6(4), 291-308 (1985).
[4]. I. A. Eltayeb and D. E. Loper, On the stability of vertical double-diffusive interfaces. Part 2: Two parallel interfaces, Journal of Fluid Mechanics, 267, 251-273 (1994).
[5]. P. G. Drazin and W. H. Reid, Hydrodynamic stability, Combridge University Press, Cambridge (1981).
[6]. H. H. Bau, Kelvin-Helmholtz instability for parallel flow in porous media: A linear theory physics of fluids, 25(10), 1719-1722, 1982.
[7]. K. Zakaria, M. A. Sirwah, and S. A. Alkharashi, Temporal stability of superposed magnetic fluids in porous media, Physic a Scripta, 77(2), 025401 (2008).
[8]. S. A. Alkharashi, Electrohydrodynamic instability of three periodic streaming fluids through porous media, Open Access Library Journal, 2, e1315 (2015).
[9]. G. M. Moatimid, Nonlinear Kelvin-Helmholtz instability of two miscible ferrofluids in porous media, ZAMP, 57, 133-159 (2006).
[10]. G. M. Moatimid, and M. A. Hassan, The instability of an electrohydrodynamic viscous liquid microcylinder buried in aporous medium; Effect of Thermosolutal Marangoni convection, Mathematical problems in Engineering, 2013, Article 1 D 416526, 14 pages (2013).
[11]. D. D. Joseph, Potential flow of viscous fluids: Historical notes, International Journal of Multiphase Flow, 32, 285-310 (2006).

[12]. G. M. Moatimid, and M. A. Hassan, Viscous potential flow of electrohydrodynamic Kelvin-Helmholtz instability through two porous layers with suction/ injection effect, International Journal of Engineering Science, 54, 15-26 (2012).
[13]. G. M. Moatimid, M. A. Hassan, and B. E. M. Tantawy, Nonlinear electrohydrodynamic Kelvin-Helmholtz instability through two porous layers with suction/ injection: viscous potential theory, Journal of Natural Sciences and Mathematics, 7(2), 129-154 (2014).
[14]. D. K. Tiwari, M. K. Awasthi, and G. S. Agrawal, Viscous potential flow analysis of magnetohydrodynamic capillary instability with heat and mass transfer, Ain Shams Engineering Journal, 6(3), 1113-1120(2015).
[15]. G. M. Moatimid, Y. O. El-Dib and M. H. Zekry, Instability analysis of a streaming electrified cylindrical Sheet through porous media, has been accepted in Pramana Journal of Physics (2018).
[16]. J. R. Melcher, Field coupled surface waves, M.I.T. Press, Cambridge M.A. (1963).
[17]. W. K. H. Panofsky and M. Phillips. Classical Electricity and Magnetism. Addison-Wesley, 2nd edition, 1962. Dover (2005).
[18]. Z. Zahreddin, E. F. El-Shehawey, On the stability of system of differential equations with complex coefficients, Indian Journal of Pure and Applied Mathematics, 19(10), 963-972, (1988).

Appendix

The coefficients that appearing in equations (4.3) and (4.4) are listed as follows:

$$f_{1j}=\frac{-1}{k\,\xi_2\xi_{(2j-1)}}(\xi_2\rho_{(2j-1)}\coth[(h-a)k]-\xi_{(2j-1)}\rho_2\coth(2ak)),\quad f_{22}=\frac{\rho_2}{k\xi_2}\operatorname{csc}h(2ak),$$

$$l_{1j}=\frac{-1}{k}\Big(\big(2k^2\mu_{(2j-1)}+\upsilon_{(2j-1)}\big)\coth[(h-a)]+\big(2k^2\mu_2+\upsilon_2\big)\coth(2ak)\Big),\ l_{22}=\frac{(2k^2\mu_2+\upsilon_2)}{k}\operatorname{csc}h(2ak),$$

$$a_{1j}=\frac{k\rho_2V_2^2}{\xi_2^2}\coth(2ak)+\frac{k\rho_{(2j-1)}V_{(2j-1)}^2}{\xi_{(2j-1)}^2}\coth[(h-a)k]+(-)^j g(\rho_2-\rho_{(2j-1)})-k^2T_{j(j+1)},$$

$$g_{1j}=-\left(\frac{V_{(2j-1)}\rho_{(2j-1)}(1+\xi_{(2j-1)})}{\xi_{(2j-1)}^2}\coth[(h-a)k]+\frac{V_2\rho_2(1+\xi_2)}{\xi_2^2}\coth(2ak)\right),$$

$$b_{1j}=\frac{k}{M}(\varepsilon_{(2j-1)}-\varepsilon_2)^2\sinh[(a-h)k]\Big((\varepsilon_2-\varepsilon_{(5-2j)})\sinh[(3a-h)k]-(\varepsilon_2+\varepsilon_{(5-2j)})\sinh[(a+h)k]\Big),$$

$$b_{22}=2\frac{k}{M}\varepsilon_2(\varepsilon_1-\varepsilon_2)(\varepsilon_2-\varepsilon_3)\sinh^2[(a-h)k],$$

$$M=\varepsilon_2(\varepsilon_1+\varepsilon_3)\cosh(2ak)\sinh[2(a-h)k]+(\varepsilon_2^2-\varepsilon_1\varepsilon_3)\sinh(2ak)-(\varepsilon_2^2+\varepsilon_1\varepsilon_3)\cosh[2(a-h)k]\sinh(2ak),$$

$$c_{1j}=-\Big(\big(2k^2\mu_{(2j-1)}+\upsilon_{(2j-1)}\big)V_{(2j-1)}\coth[(h-a)k]+(2k^2\mu_2+\upsilon_2)V_2\coth(2ak)\Big),$$

$$g_{22}=\frac{V_2\rho_2(1+\xi_2)}{\xi_2^2}\operatorname{csc}h(2ak).\ c_{22}=V_2(2k^2\mu_2+\upsilon_2)\operatorname{csc}h(2ak),\ a_{22}=-\frac{k\rho_2V_2^2}{\xi_2^2}\operatorname{csc}h(2ak),$$